

## Influence of the structure and morphology of $\text{MnO}_2$ on the electrochemical performance of supercapacitor systems

G. D. Ivanova<sup>1\*</sup>, A. E. Stoyanova<sup>1</sup>, L. S. Soserov<sup>1</sup>, D. G. Kovacheva<sup>2</sup>,  
D. B. Karashanova<sup>3</sup>

<sup>1</sup> Institute of Electrochemistry and Energy Systems – Bulgarian Academy of Sciences,  
G. Bonchev Street, bl.10, 1113 Sofia, Bulgaria

<sup>2</sup> Institute of General and Inorganic Chemistry – Bulgarian Academy of Sciences,  
G. Bonchev Street, bl.11, 1113, Sofia, Bulgaria

<sup>3</sup> Institute of Optical Materials and Technologies – Bulgarian Academy of Sciences,  
G. Bonchev Street, bl.109, 1113 Sofia, Bulgaria

Received October, 2016; Revised December, 2016

In the present work three type nanosized manganese oxides are structurally and morphologically characterized using X-Ray diffraction, Scanning electron microscopy and Transmission electron microscopy. A supercapacitor cells are composed by a positive electrode - a composite with teflonized acetylene black (XC-35) and 50 wt.%  $\text{MnO}_2$ , negative electrode of activated carbon (Cabot CGP Super,  $1800 \text{ m}^2\text{g}^{-1}$ ) with addition of polytetrafluoroethylene (PTFE) and carbon black (Cabot SC2) and alkaline electrolyte (7M KOH with addition of  $35 \text{ g l}^{-1}$  LiOH) and subjected to electrochemical tests at different current loads ( $30\text{--}420 \text{ mA g}^{-1}$ ) and prolong cycling (up to 350 cycles) using Arbin BT2000 apparatus.

The results show that the structure and morphology of  $\text{MnO}_2$  play a significant role on the supercapacitor performances. The highest discharge capacity ( $180\text{--}200 \text{ F g}^{-1}$ ) and most stable cycle ability at prolong cycling are observed for a single phase  $\text{MnO}_2$  with akhtenskite type structure and crystallites sizes about 5–6 nm.

**Key words:** supercapacitors, manganese dioxide, electrode materials, structure, morphology.

### INTRODUCTION

Supercapacitors have a lower energy density, but a higher power density, and longer shelf and cycle life than batteries [1]. Due to these properties, supercapacitors have potential applications in various power and energy systems, such a hybrid vehicles, portable computers, mobile phones, micro-grids and others. In addition, supercapacitors possess much potential to serve as a device energy buffer in the data storage industry [2].

In order to improve the energy density at long life of energy source are developed hybrid electrochemical systems (e.g. asymmetric supercapacitors) at which both electrodes are made of different materials. The supercapacitors require porous and stable electrodes. Carbon-based active materials (AC) are the most widely used electrode materials

in these systems thanks to their physical and chemical properties [3].

Transition metal oxides, such as hydrous  $\text{RuO}_2$ , NiO and  $\text{MnO}_2$  have been identified as possible composite materials for a high power and higher energy density supercapacitor [4–7]. They represent a type of attractive material with high specific capacitance, wide operational potential window and stability through charge–discharge cycling. Ruthenium oxide ( $\text{RuO}_2$ ), as an early example, can deliver relatively constant and appreciable capacitance of  $600\text{--}1000 \text{ F g}^{-1}$  with a potential window of 1.0–4.0 V. However, the rarity of ruthenium in the earth's crust and hence the high market price of  $\text{RuO}_2$  limits its applications mostly in military and aerospace [8].

Manganese, as the twelfth most abundant element on the earth, is an inexpensive material with various oxidation states. Manganese oxides ( $\text{MnO}_x$ ) are a class of environmentally friendly material compared with other metal oxides, only harmful by excessive inhalation or imbibing. Throughout the years,  $\text{MnO}_x$

\* To whom all correspondence should be sent:  
E-mail: galia\_ivanova2000@yahoo.co.uk

in various forms has been widely studied as the electrode materials in various energy storage systems, such as alkaline batteries, lithium ion batteries and supercapacitors and has been proven to be a reliable electrode material with high performance [9].

Manganese dioxide is demonstrated to be one of the most promising electrode materials for supercapacitors because of such superior characteristics as large specific capacitance, environmental benignity nature, natural abundance and low cost [10]. It was found that the textural characteristics, crystal forms and ion conductivity of MnO<sub>2</sub> strongly influence the electrochemical performances [11, 12]. Because of this there are a lot of reports on MnO<sub>2</sub> preparation technologies, such as a co-preparation method, a thermal decomposition method, a sol-gel method and so on [13–16].

Nano-structured MnO<sub>2</sub> has the advantages of large specific area, wider charge/discharge potential range, higher specific capacitance, and good environmental compatibility, which attracts many attentions in the world as electrode material for supercapacitors in recent years. One powerful and straightforward approach is to incorporate uniform MnO<sub>2</sub> nanostructures into an electrical conductive substrate, which is demonstrated to be an effective method to improve the electrochemical performance [17–22].

The effect of MnO<sub>2</sub> loading on the electrochemical performance was investigated by cyclic voltammeter and galvanostatic charging/discharging technique. The results showed that an ultra thin MnO<sub>2</sub> deposits were indispensable to achieve better electrochemical performance. The theoretical specific capacitance of MnO<sub>2</sub> is estimated to be 1370 Fg<sup>-1</sup>. This ultrahigh value has only been obtained in nanoscale MnO<sub>2</sub> (1380 Fg<sup>-1</sup>) [23], however, the capacitance decreases rapidly with the increase in the MnO<sub>2</sub> mass.

In the present work the effect of the structure and morphology of three type nanoscale manganese dioxide on its characteristics as electrode material in hybrid supercapacitors is discussed. The investigated samples were characterized by means of physicochemical (X-Ray diffraction, Scanning electron microscopy and Transmission electron microscopy) and electrochemical (charge/discharge galvanostatic cycling) methods.

## EXPERIMENTAL

For the purposes of this study two types commercial nanoscale MnO<sub>2</sub> (Faradizer FW and Faradizer FM), Sedema company, Belgium and one type MnO<sub>2</sub> produced from company Fluka, USA are tested. Faradizer type manganese oxides are inves-

tigated previously as electrode material in lithium-ion batteries and showed a good electrochemical properties [24, 25].

These materials are structurally characterized by X-diffraction (XRD) method. The powder X-ray diffraction patterns are collected in the range from 10 to 80° 2θ with a constant step of 0.02° 2θ angle on Bruker D8 Advance diffractometer with Cu Kα radiation and Lynx Eye detector. Phase identification was performed with the Diffractplus EVA using ICDD-PDF2 Database. The powder diffraction patterns are evaluated with the Topas-4.2 software package using the fundamental parameters peak shape description including appropriate corrections for the instrumental broadening and diffractometer geometry.

The surface morphology of the electrode materials are examined by JEOL JSM-5510 and JEOL Superprobe 733 scanning electron microscope (SEM) and JEOL 2100 Transmission electron microscope (TEM). The specimens are prepared by grinding the samples in an agate mortar and dispersing them in ethanol by ultrasonic treatment for 5 min. A droplet of each suspension is dropped on standard Cu grid, covered by amorphous carbon film and dried in pure atmosphere at room temperature.

The hybrid supercapacitor cell is composed by a positive electrode – a composite with teflonized acetylene black (XC-35) and different types MnO<sub>2</sub> (50 wt.%), and a negative electrode of activated carbon (Cabot CGP Super, 1800 m<sup>2</sup>g<sup>-1</sup>) with addition of carbon black (Cabot SC2) and polytetrafluorethylene (PTFE) as a binder. PTFE is added previously to the activated carbon under standardized methodology. The formed sheet electrodes (surface area 1,75 cm<sup>2</sup>) are dried at 140 °C for 12 hours and pressed under pressure of 20 MPa. The obtained electrodes are soaked in the electrolyte (7M KOH with 35 gl<sup>-1</sup> LiOH) under vacuum and then mounted in a coin-type cell with Viledor 700/18F separator and filled with electrolyte. The capacitor cells are subjected to galvanostatic charge-discharge cycling using an Arbin Instrument System BU-2000 [26]. The test program is carried out at constant current mode at different current load (from 30 to 360 mA g<sup>-1</sup>) at 25 cycles and room temperature. Some cells are subjected to continuous cycling charge/discharge at current rate 60 mA g<sup>-1</sup> up to 350 cycles.

The value of the specific capacity  $C$  is obtained from the charge-discharge cycling measurements according to the following equation [27]:

$$C = 4 I \Delta t / m \Delta V \quad (1),$$

where  $I$ ,  $\Delta t$ ,  $\Delta V$  and  $m$  are respectively, the constant current applied, charge/discharge time, voltage range and the total mass of the electrode material.

## RESULTS AND DISCUSSION

### Physicochemical characterization

The results of X-ray diffraction characterization show that the investigated manganese oxides differ in their phase composition and size of the crystallites.  $MnO_2$ , produced from Fluka company contains a single phase  $MnO_2$  – akhtenskite type structure with crystallites sizes about 5–6 nm. The both other samples  $MnO_2$  FW and  $MnO_2$  FM are composites of two type structures – akhtenskite and pyrolusite and Ni, respectively with larger crystalline sizes and a non-homogeneous structure (Fig. 1, Table 1).

The crystallite sizes of different  $MnO_2$  samples are determined on the basis of broadening of diffraction peaks and are shown in Table 1.

In order to clarify the role of morphology in electrochemical performance, SEM and TEM are utilized to observe the morphology of the different types Mn-oxides.

The SEM images of the samples reveal a great difference in the morphological characteristics and correspond very well with X-ray diffraction patterns. From Fig. 2c it can be seen that  $MnO_2$  FM shows a strongly inhomogeneous structure with a large difference in crystal sizes and thus less developed surface area.

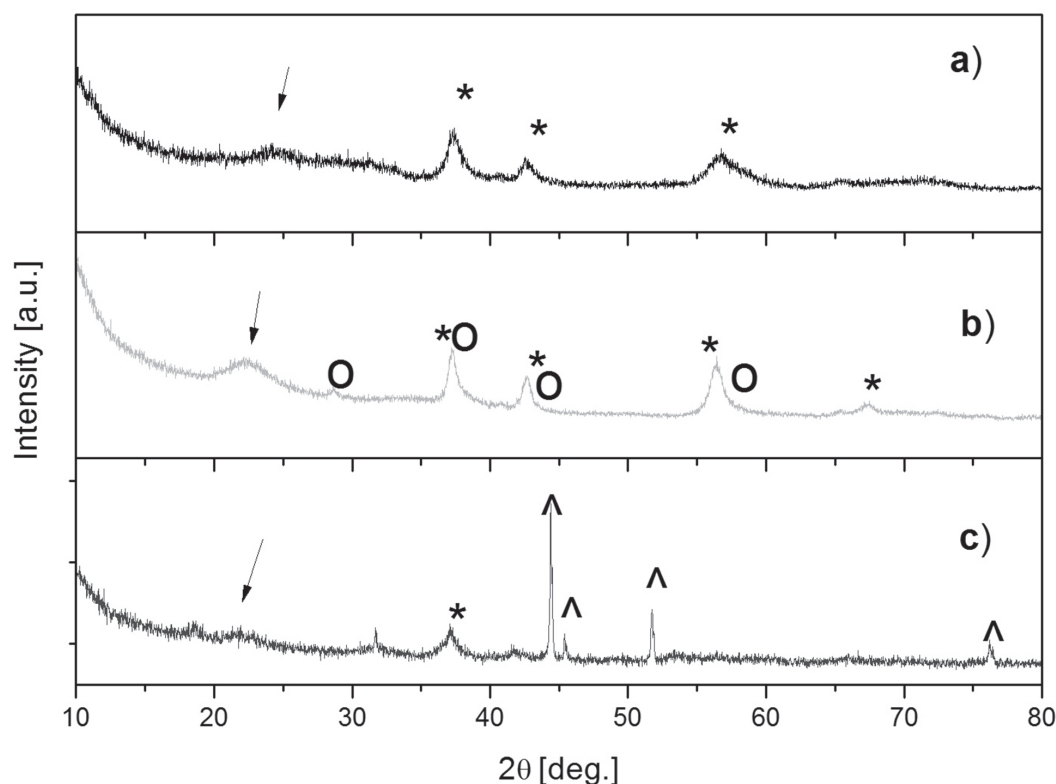


**Fig. 1.** Powder XRD patterns of different manganese oxides: a)  $MnO_2$ , b)  $MnO_2$  FW and c)  $MnO_2$  FM. The different phases were denoted as follows: \* –  $\alpha$ - $MnO_2$  akhtenskite, o –  $MnO_2$ , pyrolusite, ^ – metallic Ni. With arrows are pointed the amorphous humps.

**Table 1.** Determined crystallite size of investigated  $MnO_2$  samples

Type	Crystallite size, nm		
	Akhtenskite	Pyrolusite	Ni
$MnO_2$	6	–	–
$MnO_2$ FW	4	14	–
$MnO_2$ FM	10	–	124

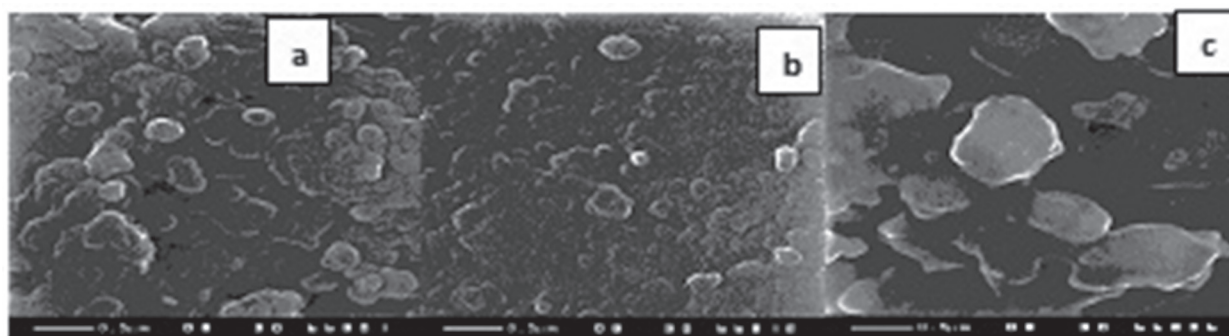


Fig. 2. SEM images of  $\text{MnO}_2$  (a),  $\text{MnO}_2$  FW (b) and  $\text{MnO}_2$  FM (c).

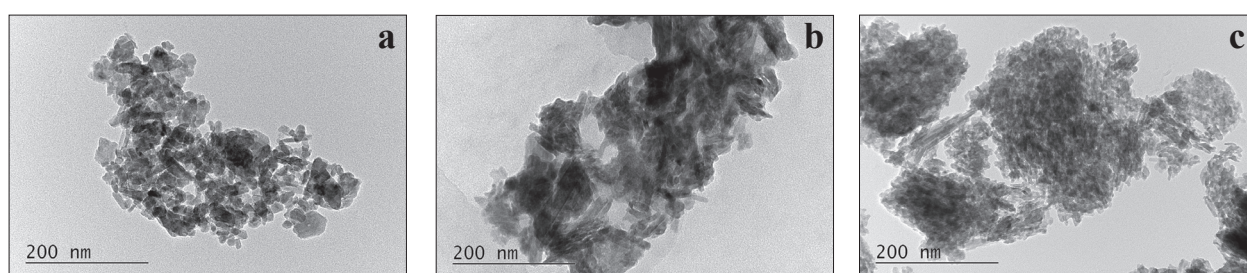


Fig. 3. TEM images of  $\text{MnO}_2$  (a),  $\text{MnO}_2$  FW (b) and  $\text{MnO}_2$  FM (c).

The TEM observation provides additional information on lattice distortion, the size and the distribution of Mn particles and in Figure 3 are displayed the TEM images of the studied  $\text{MnO}_2$  samples.

The TEM micrographs of  $\text{MnO}_2$  (Fig. 3a) show that the particles are nanosized and homogeneous in size, while in  $\text{MnO}_2$  FW and  $\text{MnO}_2$  FM samples (Figs. 3b and 3c) dominate large formations, separated by layered structures and small clusters. There is also a significant difference in the form of crystalline particles. The micrographs of both samples ( $\text{MnO}_2$  and  $\text{MnO}_2$  FW) show needle-shaped particles, while the  $\text{MnO}_2$  FM consists of round particles (Fig. 3).

In our previous study the physicochemical characteristics of used activated carbon Cabot CGP Super are examined in detail and it is found that this material has a very high specific surface area ( $1800 \text{ m}^2\text{g}^{-1}$ ) and small particles clusters [28].

#### Electrochemical characterization

The electrochemical performance of the two-electrode hybrid capacitor cells are studied by charge-discharge cycling test and are presented in Figures 4–6.

Figure 4 gives the dependences of the discharge capacitance as a function of discharge current density for studied composite electrodes fabricated by using three types  $\text{MnO}_2$ . It can be seen the signifi-

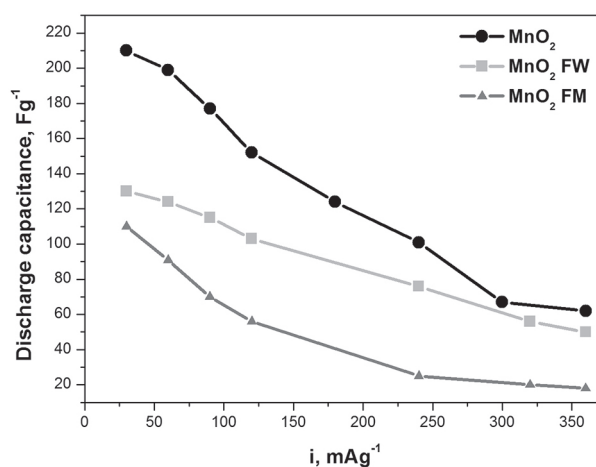


Fig. 4. Dependence of the discharge capacitance of hybrid supercapacitor cells with different types  $\text{MnO}_2$  on the current loads.



cant role on the structure and morphology of the active composite material on its electrochemical performances. The analysis of the cycling behaviors shows that all three hybrid supercapacitor cells demonstrate good reproducibility of the charge/discharge process and high specific discharge capacity, which is best expressed using  $\text{MnO}_2$ . Substantially lower capacity indicates the cell with  $\text{MnO}_2$  FM, which possesses inhomogeneous structure with very large crystal sizes.

To illustrate still better the effect of the structure on the metal oxide in composite electrode on its electrochemical performance, Figure 5 shows the charge-discharge profile curves of all studied samples fabricated in electrodes with different  $\text{MnO}_2$ , measured at  $60 \text{ mA g}^{-1}$ . The electrodes with  $\text{MnO}_2$  and  $\text{MnO}_2$  FW active material show that approximately linear voltage varies with time during both charge and discharge process which indicates that these oxides with such a structure and morphology behave as capacitors and have a good cycling stability. The electrode with  $\text{MnO}_2$  demonstrates the lowest voltage drop during the discharge process, giving high values of charge/discharge efficiency [2].

The cycle life of the investigated hybrid capacitors cells is also illustrated in Figure 6, where the specific discharge capacitances of electrode materials are given as a function of cycle number. This test of cycle life is performed under constant current load ( $60 \text{ mA g}^{-1}$ ) conditions.

The analysis of the cycling behaviors shows that the  $\text{MnO}_2$  – akhtenskite type structure demonstrates the highest discharge capacity (around  $180 \text{ Fg}^{-1}$ ) and most stable cycleability at prolong cycling. The both other structures of  $\text{MnO}_2$  also exhibit a long

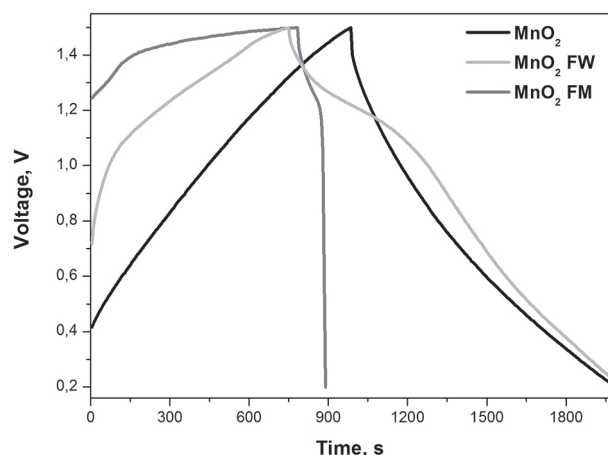


**Fig. 5.** Galvanostatic charge and discharge curves of hybrid supercapacitor cells with different types  $\text{MnO}_2$  at current load of  $60 \text{ mA g}^{-1}$ .

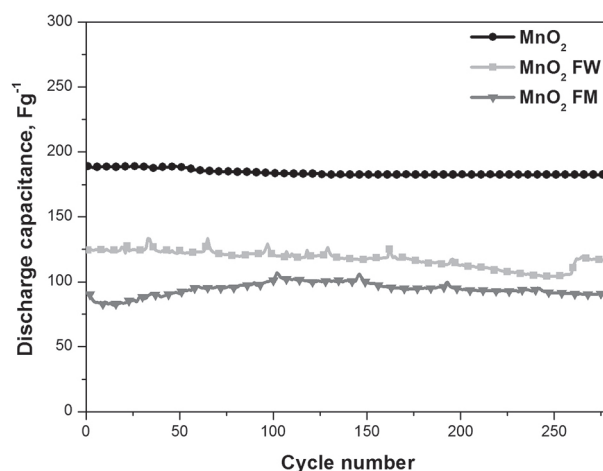


**Fig. 6.** Dependence of the specific capacitance of hybrid supercapacitor cells with different types  $\text{MnO}_2$  on the number of cycles at current rate  $60 \text{ mA g}^{-1}$ .

cycle life under shallow depth of discharge, but significantly worse capacitor properties (especially  $\text{MnO}_2$  FM).

## CONCLUSION

In this paper, three type nanosized manganese oxides are structurally and morphologically characterized and investigated as composite electrode materials in hybrid supercapacitors in alkaline electrolyte. The highest discharge capacity ( $180\text{--}200 \text{ Fg}^{-1}$ ) and most stable cycle ability at prolong cycling demonstrates  $\text{MnO}_2$  which contains a single phase akhtenskite type and homogenous structure with crystalline sizes about  $5\text{--}6 \text{ nm}$ . The others two tested oxides (Faradizer FW and FM) with two phase structure and significant difference in the crystal sizes and pronounced lack of homogeneity (especially manganese  $\text{MnO}_2$  FM) demonstrate stable, but considerably lower discharge capacitance. The obtained results confirm the positive effect of application of  $\text{MnO}_2$  with defined structure and morphology as active electrode material in supercapacitors.

**Acknowledgement:** The financial support of the BNSF under project DFNP-42/21.04.2016 and DFNI E02/18-2014 are gratefully acknowledged.

## REFERENCES

1. A. Burke, *J. Power Sources*, **91**, 37 (2000).
2. Jun Li, H. Wang, Q. Huang, S. Gamboa, P. Sebastian, *J. Power Sources*, **160**, 1501 (2006).

3. T. Cottineau, M. Toupin, T. Delahaye, T. Brousse, D. Bélanger, *Appl. Phys.*, **A 82** (4), 599 (2006).
4. C. Portet, P. L. Taberna, P. Simon, E. Flahaut, C. Laberty-Robert, *Electrochim. Acta*, **50**, 4174 (2005).
5. W. C. Chen, C. C. Hu, C. C. Wang, *J. Power Sources*, **125**, 292 (2004).
6. P.R. Kalakodimi, M. Nono, *Electrochem., Solid State Lett.*, **7–11**, 425 (2004).
7. W. Gui-Xin, Z. Bo-Lan, Y. Zuo-Long, *Solid State Ionics*, **176**, 1169 (2005).
8. B. E. Conway, *Electrochemical supercapacitors: scientific fundamentals and technological applications*, Kluwer Academic/Plenum Publishers, New York, 1999.
9. A. A. Francis and C. Forsyth: available at: <http://rais.ornl.gov/tox/profiles/mn.shtml>.
10. W. Wei, X. Cui, W. Chen, D. G. Ivey, *Chem. Soc. Rev.*, **40**, 1697 (2011).
11. S. Devaraj, N. Munichandraiah, *J. Phys. Chem.*, **C 112**, 4406 (2008).
12. O. Ghodbane, J. L. Pascal, F. Favier, *ACS Appl. Mater. Interfaces*, **1**, 1130 (2009).
13. N. R. Reddy, G. R. Reddy, *J. Power Sources*, **124**, 330 (2003).
14. Y. U. Jeong, A. Mantiram, *J. Electrochem. Soc.*, **149**, 1419 (2002).
15. X. Y. Chen, X. Li, Y. Jank, *Solid State Commun.*, **136**, 94 (2005).
16. J. Li, X. Y. Wang, Q. H. Huang, S. Gamboa, P. J. Sebastian, *J. Power Sources*, **160**, 1501 (2006).
17. S. C. Pang, M. A. Anderson, T. W. Chapman, *J. Electrochem. Soc.*, **147**, 444 (2000).
18. R. N. Reddy, R. G. Reddy, *J. Power Sources*, **132**, 315 (2004).
19. Y. S. Chen, C. C. Hu, Y. T. Wu, *J. Solid State Electrochem.*, **8**, 467 (2004).
20. K. R. Prasad, N. Miura, *Electrochem. Commun.*, **6**, 1004 (2004).
21. Y. Kuzuoka, C. Wen, J. Otomo, M. Ogura, T. Kobayashi, K. Yamada, H. Takahashi, *Solid State Ionics*, **175**, 507 (2004).
22. Chen Ye, Zhang Mi Lin, Shi Zhao Hui, *J. Electrochem. Soc.*, **15**, A 1272 (2005).
23. M. Toupin, T. Brousse, D. Belanger, *Chem. Mater.*, **16**, 3184 (2004).
24. V. Manev, N. Ilchev, A. Nassalevska, *J. Power of Sources*, **25**, 167 (1989).
25. N. Ilchev, V. Manev, *J. Power of Sources*, **35**, 175 (1991).
26. M. Mladenov, K. Alexandrova, N. Petrov, B. Tsynsarski, D. Kovacheva, N. Saliyski, R. Raicheff, *J. Solid State Electrochem.*, **17**, 2101 (2013).
27. M. Stoller and R. Ruoff, *Energy & Environment Sci.*, **3**, 1294 (2010).
28. Ch. Girginov, L. Stoyanov, S. Kozhukharov, A. Stoyanova, M. Mladenov, R. Raicheff, in: *Chemical Technologies (Proceedings of RU&SU'15, Ruse, 2015)*, University of Ruse Angel Kanchev Proceedings, 2015, **54**, 10.1, p. 89.

## ВЛИЯНИЕ НА СТРУКТУРАТА И МОРФОЛОГИЯТА НА MnO<sub>2</sub> ВЪРХУ ЕЛЕКТРОХИМИЧНИТЕ ХАРАКТЕРИСТИКИ НА СУПЕРКОНДЕНЗАТОРНИ СИСТЕМИ

Г. Д. Иванова<sup>1\*</sup>, А. Е. Стоянова<sup>1</sup>, Л. С. Сосеров<sup>1</sup>, Д. Г. Ковачева<sup>2</sup>, Д. Б. Карашанова<sup>3</sup>

<sup>1</sup> *Институт по Електрохимия и Енергийни Системи – Българска Академия на Науките*

<sup>2</sup> *Институт по Обща и Неорганична Химия – Българска Академия на Науките*

<sup>3</sup> *Институт за Оптични Материали и Технологии – Българска Академия на Науките*

Постъпила октомври, 2016 г.; приета декември, 2016 г.

(Резюме)

В представената работа структурно и морфологично са охарактеризирани три типа наноразмерен манганов оксид с помощта на рентгенова дифракция, сканираща електронна микроскопия и трансмисионна електронна микроскопия.

Суперкондензаторните клетки са съставени от положителен електрод – композит на основата на етефлонизиран въглен сажди (XC-35) и 50 тегл.% MnO<sub>2</sub> и отрицателен електрод, съставен от активен въглен (Cabot CGP Super, 1800 m<sup>2</sup>g<sup>-1</sup>) с добавка на политетрафлуоретилен (ПТФЕ) и въглен сажди (Cabot SC2). Използван е алкален електролит (7M KOH с 35 g l<sup>-1</sup> LiOH) и така асемблираните клетки са подложени на електрохимични изпитания при различни токови натоварвания (30–420 mA g<sup>-1</sup>) и продължително циклиране (до 350 цикъла) с помощта на електрохимична система Arbin VT2000.

Резултатите показват, че структурата и морфологията на MnO<sub>2</sub> играят важна роля за характеристиките на суперкондензаторите. Най-висок разряден капацитет (180–200 F g<sup>-1</sup>) и най-стабилна циклируемост при продължително циклиране се наблюдава за еднофазен MnO<sub>2</sub> с актенски тип структура и размери на кристалитите 5 nm.